Investigating the Length, Area and Volume Measurement Accuracy in UAV-Based Oblique Photogrammetry Models produced with and without Ground Control Points

Erdem Maraş (erdem.maras@samsun.edu.tr)
Samsun University
Mohammad Nasery
Ondokuz Mayıs University

Research Article

Keywords: Oblique photogrammetry, Ground Control Points, GCP, UAV

Posted Date: April 9th, 2021

DOI: https://doi.org/10.21203/rs.3.rs-396298/v1

Version of Record: A version of this preprint was published at International Journal of Engineering and Geosciences on February 21st, 2022. See the published version at https://doi.org/10.26833/ijeg.1017176.

Abstract

This study was aimed to investigate the performance and sensitivity of a 3D photogrammetric model generated without GCPs (Ground Control Points). To see if the models with no GCPs show the accuracy in every types of terrain as well as climate or metrological conditions, two separate studies are done in two areas with different characteristics such as Altitude, slope, topography, and meteorological varieties. The study areas were initially modelled with GCPs and later without GCPs. Furthermore, some of the dimensions and areas within the modelled area were measured using terrestrial techniques (with GPS/GNSS) for accuracy analysis. After modelling within the areas with and without GCPs, different territories with different slope and geometric shapes were selected. Various measurement in terms of length, area and volume carried out over the selected territories within both model (generated with and without GCPs) of each 2 studies. The datasets obtained as results of measurements were compared to each other and the measurements carried out over the models produced with GCPs were accepted as true values. Results from length measurement provided various level of success. First study area exhibited very promising results in length measurement with a relative error of less than 1% and RMSE (Root Mean Square Error) of 0.139m. In the case of area measurement, in the first study area (Sivas), a minimum relative error of 0.04% and a maximum relative error of 1.05% with a RMSE of 1.264 m² is obtained. In the second study areas (Artvin) for area measurement a minimum relative error of 0.56% and a maximum relative error of 5.27% with a RMSE of 1.76m² is achieved. And finally, in the case of volume measurement, for fist study area (Sivas) a minimum relative error of 0.8% and a maximum relative error of 6.8% as well as 2.301 m³ is calculated. For second study area (Artvin) minimum relative error for volume measurement is 0.502% as well as maximum relative error is 2.01% with a 7.061m³ RMSE.

1. Introduction

Photogrammetry and especially digital photogrammetry is a versatile tool for aerial surveys and is rapidly becoming the tool of election to generate 3D realistic models from 2D photos for different engineering projects. 3D modelling via Digital photogrammetry is based on combination of vertical and inclined imagery. Oblique photogrammetry offers improved capabilities for 3D reconstruction of different surfaces and terrains. 3D models obtained via oblique photogrammetry have widespread use in different engineering fields and this application area is expanding day by day due to recent advances in technology, hardware, and software development. Nowadays Digital photogrammetry has numerous potential applications in areas such as surveying, civil engineering, urban planning, architecture, archeology, mining, monitoring mass movements, industry, urban management, agriculture, real estate etc.

Digital photogrammetry or three-dimensional (3D) mapping which is the most famous discipline of the digital age is expanding quickly overall the world majorly due to low-cost facility for data acquisition and fast workflow. Basically, UAV photogrammetry makes possible three-dimensionally (3D) reconstruction of objects via two-dimension (2D) photos. Besides, a model produced via oblique photogrammetry does not aims just viewing and displaying but it also provides accurate geometric and spatial information about the object. In oblique photogrammetry UAV (unmanned aerial vehicle) also known as drone are used for aerial imagery. Recently UAV photogrammetry is used in different areas such as cultural heritage documentation

[1, 2] agriculture [3, 4] architectural restoration [5, 6], archeology [7, 8], mining [9, 10], monitoring coastal habitats [11], urban and infrastructure planning [12, 13]. The old challenging methods for data acquisition are eliminated by photogrammetry. Sense 2D cadaster information does not meet today's needs, the world is moving into the 3D cadaster system, as its name clearly shows that in this application third dimension's information is needed for and such information could be supplied just with oblique photogrammetry [14]. Three-dimensional photogrammetric modeling play an important role in designing three-dimensional city modeling as well as in urban management especially during the planning stage it helps the urban planners to make optimum planes for the city.

In another research [15] states that since two dimensional cadaster is insufficient to solve the problems occurring due to lack of third dimension reveals the need for 3D cadaster implementation. [16] used the UAV-based oblique photogrammetry for purpose of determining the characteristics of city trees and modeled a specific area for this purpose and determined the characteristics of city trees through the three-dimensional model. In [17] for obtaining better 3D city models they used a new method in which the aerial images are combined to the terrestrial images and at the results they obtained good 3D city models with properly geometries of the buildings. in a research namely Quantifying uncertainties in snow depth mapping from structure from motion photogrammetry in an alpine area, used the structure from motion photogrammetry to characterize uncertainties in snow depths spatially [18]. For this purpose, a study was conducted in the Combe de Laurichard which is located in the French Alps. Two different time of June 1st and October 5th, 2017 was chosen (one snow-on and one snow-off condition) for aerial data acquisition and two DEM (digital elevation model) from two datasets were made and compared, in this study a method was presented for calculating a spatially varying estimate of snow depth precision and detection limits using UAV repeated surveys. In their study [19] namely High-accuracy UAV photogrammetry of ice sheet dynamics with no ground control points, presented the application of an alternative SFM- MVS (structure from motion-multi view stereo) geolocation method named as GNSS-supported aerial triangulation, in this method an onboard carries-phase GNSS receiver to georeference SFM-MVS (structure from motion-multi view stereo) point cloud which significantly reduced the need for GCP (ground control points). Considered various flight configurations such as linear strips, radial strips and curved strips; the obtained various dataset are evaluated in terms of density of the extracted point clouds and also distance between the reconstructed surface and control points are evaluated [20].

2. Definition Of Problem

As a matter of fact, Ground Control Points (GCPs) are one of mandatory factors for generating an accurate photogrammetric model, but what if GCPs (Ground Control Points) cannot be marked due to location inaccessibility such as lands with high slope (Canyon) and vertical structures (dam body), insufficient project budget, areas with landslide risks or some other hazardous field situations such as glaciological environment. Modeling such lands and structures with GCP is sometimes impossible or need a huge amount of budget. Should a photogrammetric model without GCP still be deemed as accurate for some engineering applications or not?

3. The Aim Of Study

The purpose of this paper is to indicate the usability of photogrammetric models generated without GCPs (ground control points) in some engineering application such as length, area, and volume measurements.

For this purpose, two different areas with different characteristics were modelled with and without GCPs. The areas and lengths are measured from orthophoto and the volumes are calculated from DEM (Digital Elevation Model).

The measurements mentioned above are done over same areas in both models produced with and without GCPs and the results are discussed in detail.

4. Material And Methods

For the data acquisition of this research a DJI Phantom 4 Pro Drone with a satellite positioning system of GPS/GLONASS with vertical hover accuracy of ± 0.1 m horizontal hover accuracy of ± 1.5 m and 20 MP (Mega Pixel) camera. DJI Terra's Oblique Mission uses 5 flight routes to capture the same amount of data as using 5 cameras simultaneously on a drone. The 5 flight routes correspond to the 5 camera headings – downward, forward, backward, leftward, and rightward.

For the measurement of GCP (Ground Control Points), GEOMAX Zenith40 type GPS/COARS is used which has 72 channels (GPS/GLONASS) with a Maximum 36 Satellite signal reciever simultaneously and the Satellite signal tracking capacity in GPS is L1, L2, L2C and in GLONASS is L1, L2. Data processing is done in the Agisoft Metashape software 1.5.2 version and datas obtained from Agisoft Metashape are also processed in MS Excel.

5. Case Study

To investigate the usability of 3D (Three- dimensional) photogrammetric models generated without GCPs (ground control points), two studies were conducted in two different provinces of Turkey with different characteristics. First one in Siva located in the south of Turkey with 1650 m. elevation (Altitude above sea level) and the second one in Artvin located in the northeast of Turkey with an elevation of 450 m. Since there is a big difference in height between two regions as well as another variety factors such as meteorological difference, slope, terrain topography and etc to investigate that, whether this principle is applicable in everywhere or not. The two areas were modelled once with GCPs and afterwards without GCPs. The data acquisition in the both areas are as follow.

5.1 Sivas

This study is presented in Fig. 1 and conducted in Shugul Canyon located in the Sivas province of Turkey. Oblique imagery of the work area is carried out and with the help of data obtained once the area is modelled with GCPs and once without GCPs and to compare the sensitivity of the two models, the length, area and volume of the same regions were measured in both models and the results were compared.

To model the area with oblique aerial photogrammetry method a DJI Phantom 4pro model UAV is used (Fig. 2). 10 well distributed GCPs (ground control points) were used to georeference the model. The measurement of GCPs was conducted with (CHC X91 GNSS) model RTK-GNSS receiver.

At the first step 9 well distributed ground control points were established in the work area, during establishing of these points, care was taken to ensure that they can be easily seen in the photos and were establish away from the natural and artificial objects such as trees and buildings that would prevent these points from appearing in the pictures (Fig. 3).

After establishing the GCPs the measurement of these points was done in Turkish National Reference System as TUREF / TM36 and (ITRF96 in universal system as EPSG: 5256) with a sensitivity of (2cm) and the obtained coordinates are given in Table 1.

Table 1
Coordinate list of ground control points

Point No	Y	X	Z
P.1	607223.539	4292394.086	1401.258
P.2	607217.702	4292407.654	1409.344
P.3	607141.923	4292390.866	1394.211
P.4	607094.008	4292376.559	1391.703
P.5	606994.953	4292671.055	1446.086
P.6	606986.964	4292597.873	1407.067
P.7	606845.780	4292703.114	1445.776
P.8	606793.686	4292683.833	1415.525
P.9	606664.304	4292784.330	1447.985

In the second step the flight plan and flight time was determined, since the work area was mountainous area so the appropriate time for flight was determined as 12:00–14:00. By selecting this time, the effect of shading that would cause errors in the photogrammetric evaluation was tried to be minimized. DJI Phantom 4Pro model UAV was used for the aerial photography, Phantom 4Pro is equipped with a 20MP camera which is able to take photos with 4K quality and also has a 1-inch sensor. DJI Phantom 4Pro model UAV is presented in Fig. 4.

The imagery was conducted with the above UAV and nadir and oblique images of the work area were obtained. The cross overlap in the imagery was 85% and forward overlap was %80, this overlap is sufficient to represent the topography and reconstruct the area virtually in three-dimension. Positions of GCPs, image overlap ratios and camera calibration are given graphically in Fig. 5. The errors of GCPs used during the photogrammetric evaluation are given in Table 2. The GCP errors calculated by the Agisoft/Metashape are given in Table 3.

Table 2
Correlation matrix calculated by the Agisoft/Metahshape

	Value	Error	F	Cx	Cy	B1	B2	K1	K2	K3	P1	P2
F	**3656.51**	0.04	1.00	0.00	0.20	-0.28	0.04	-0.21	0.25	0.23	0.00	-0.19
Cx	**-4.57**	0.08		1.00	0.01	-0.02	0.04	0.01	0.00	0.00	0.94	-0.01
Cy	**18.41**	0.06			1.00	-0.21	0.00	-0.03	0.02	-0.02	0.00	0.85
B1	**-7.25**	0.02				1.00	0.02	-0.02	0.00	0.00	-0.01	0.06
B2	**0.36**	0.02					1.00	0.00	0.00	0.00	-0.12	0.01
K1	**0.01**	0.01						1.00	-0.97	0.91	0.00	-0.04
K2	**-0.01**	0.01							1.00	-0.97	0.91	0.02
K3	**0.02**	0.01								1.00	0.00	-0.02
P1	**-0.01**	0.01									1.00	-0.01
P2	**-0.01**	0.01										1.00

Table 3
GCP errors calculated by the Agisoft/Metashape

Label	X error (cm)	Y error (cm)	Z error (cm)	Total (cm)	Image (pix)
point 1	1.273	1.163	-2.676	3.184	0.320 (17)
point 2	-0.265	-1.345	1.950	2.384	0.299 (21)
point 3	-2.428	1.455	2.572	3.825	0.333 (15)
point 4	1.162	-1.346	-1.782	2.518	0.198 (22)
point 5	0.637	0.363	1.899	2.036	0.117 (5)
point 6	-0.113	-0.228	-1.186	1.213	0.201 (17)
point 7	-0.694	-0.402	0.301	0.858	0.087 (5)
point 8	0.479	-0.046	-0.851	0.977	0.067 (6)
point 9	0.017	0.190	0.491	0.527	0.063 (7)
Total	**1.058**	**0.912**	**1.727**	**2.221**	**0.246**

Afterwards, the obtained aerial photographs were subjected to photogrammetric evaluation and the measured coordinates of GCPs were also used during the evaluation. Finally, geometry of the subject area has been reconstructed formally and computationally in virtual form. As a result of the evaluation, a dense cloud including 8,193,681 points with global coordinates, 3D model, orthophoto and digital elevation model were obtained as shown in Fig. 6.

After the 3D model was generated with GCPs, once again 3D model of the work area was generated without GCPs.

5.2 Artvin

This study was conducted in the Artvin dam built on the Çoruh Riverwhich is located in the Artvin province of Turkey (Fig. 7). A 3D model of the area is generated by oblique photogrammetry, once with and once without GCP.

For modelling this work area via aerial photogrammetry method a DJI Phantom 4pro model UAV was used. 5 GCPs (ground control points) were used to georeference the model. The measurement of GCPs was conducted with TRIMBLE R6 GPS (CORS/GNSS) receiver (Fig. 8). The coordinates of GCPs were measured in Turkish National Reference System as TUREF / TM42 (3 Degree) and (ITRF96 in universal system as EPSG: 5258) with a sensitivity of **(2cm)** and the obtained coordinates are given in Table 4.

Table 4
GCP coordinate list

Point NO	Y	X	Z
P1	480173.041	4534136.386	408.183
P2	480193.098	4534080.037	395.799
P3	480188.260	4533962.940	397.686
P4	480112.801	4534002.926	442.610
P5	480095.596	4533966.277	446.039

The imagery was conducted with the UAV in accordance with photogrammetric principles and as a result nadir and oblique images were obtained. The cross overlap in the imagery was 85% and forward overlap was %80, this overlap is sufficient to represent the topography and reconstruct the area virtually in three-dimension. GCP positions and image overlaps are given in the Fig. 9.

Positions and errors of GCPs used during the photogrammetric evaluation, image overlap, and camera calibration coefficients and correlation matrix are given graphically in Fig. 9. The correlation matrix is given in the Table 5. The GCPs position errors are also calculated and are given in Table 6.

Table 5
Correlation matrix calculated by the Agisoft/Metahshape

	Value	Error	F	Cx	Cy	B1	B2	K1	K2	K3	P1	P2
F	**3649.93**	0.05	1.00	0.01	0.35	-0.09	0.05	-0.33	0.34	-0.31	-0.07	0.06
Cx	**-3.28**	0.06		1.00	0.12	0.03	0.04	0.01	-0.02	0.02	0.69	-0.23
Cy	**16.63**	0.06			1.00	-0.06	0.06	-0.03	0.01	0.00	0.32	-0.31
B1	**-0.28**	0.02				1.00	0.01	0.01	-0.02	0.02	0.01	-0.01
B2	**0.21**	0.02					1.00	0.00	0.00	0.00	-0.10	0.03
K1	**0.01**	0.01						1.00	-0.97	0.93	0.01	-0.01
K2	**-0.04**	0.01							1.00	-0.99	-0.02	0.01
K3	**0.07**	0.01								1.00	0.02	-0.01
P1	**-0.01**	0.01									1.00	0.79
P2	**-0.01**	0.01										1.00

Table 6
GCPs position errors given by the Agisoft/Metashape

Label	X error (an)	Y error (an)	Z error (an)	Total (cm)	Image (pix)
P.l	-0.93064	-1.11915	1.23013	1.90573	0.321 (18)
P.2	-0.68080	0.83722	0.64880	1.25912	0.206 (21)
P.3	1.10243	-0.46048	-0.47225	1.28468	0.425 (14)
P.4	-0.78656	1.07360	-0.71107	1.50895	0.543 (8)
P.5	-0.61781	1.47969	1.62688	2.28427	0.245 (32)
Total	**0.84206**	**1.04953**	**1.03049**	**1.69484**	**0.320**

Afterwards, the obtained aerial photographs were processed in accordance to photogrammetric principles, the measured coordinates of GCPs were also used during the photogrammetric process of images. Finally topography of the area has been reconstructed in three dimension with its global position. As a result of process, a dense cloud including 18,958,130 points with global coordinates, 3D model, orthophoto and digital elevation model were obtained as shown in Fig. 10.

After reconstructing the work area virtually in three dimensions using GCPs, once 3D model was generated without GCPs.

6. Finding And Examination

In this section an accuracy assessment is initially done for models generated with GCPs. Afterwards a comparison study is done among the final 3D models (one with GCPs and other without GCPs) obtained from photogrammetric process. Length, area and volume measurements are selected as comparison criteria. These measurements are done for different areas over models generated with GCPs and afterwards over models without GCPs and at the end these results are compared to the measurement of the same areas done with terrestrial method (GPS/GNSS) the results are compared in details.

6.1 Assessment of Length, Area and Volume Measurement

6.1.1 First Study Area (Sivas) Experimental Studies

Length, area, and volume measurement of areas with different geometric shapes and slopes are carried out for first study area.

6.1.2 Length measurement for accuracy analyse of model

Initially two areas are selected for the accuracy analysis of both models, a length measurement is done for those areas with the terrestrial method (using RTK (Real Time Kinematic/GNSS)) and afterwards same areas are measured in both models (model with GCPs and model without GCPs) and. The results of the measurements are given in Table 7.

Table 7
Length measurements obtained with different methods

Area Name	Refference (With GPS) (m)	With GCPs (m)	Without GCPs (m)	*RMSE(mm)*	Relative Error %
1	13.830	13.817	13.804	0.020	0.14
2	14.770	14.765	14.792	0.016	0.11

As seen in the Table 4 our model is sensitive enough. Because the measurements are close enough to the data obtained with RTK/GNSS. On this basis the model generated with GCPs is accurate enough and since we could not measure all investigation areas with terrestrial method so in this study the data obtained from model with GCPs are accepted as true values and the other data (obtained from model without GCPs) are compared to this data. Different features are measured within both models as shown in Fig. 11.

After the model accuracy was confirmed, measurements in areas with different shapes are done in both models. The measurements are given in Table 8 and are compared as well. Measurements done in two models are graphically indicated as shown in Fig. 12.

Table 8
Length measurements obtained from two models of Sivas for the same areas

First Study (Sivas) Lenght Measurements					
Area Type	**With GCPs(m)**	**Without GCPs(m)**	**Δi(m)**	**Relative Error %**	**RMSE(m)**
Flat Areas	72.418	72.470	-0.052	0.100	**0.139**
	60.518	60.558	-0.040	0.100	
	55.466	55.424	0.042	0.100	
	253.182	253.083	0.099	0.040	
Inclined Areas	69.644	69.746	-0.102	0.150	
	61.672	61.541	0.131	0.210	
	98.036	98.230	-0.194	0.200	
Rocky Areas	238.598	238.346	0.252	0.110	
	47.994	47.821	0.173	0.360	
		mean	**0.121**	**0.126**	

6.1.3 Area Measurements for Sivas

In order to observe the usability of the model produced without GCPs in the case of area measurement, 5 areas with different features are measured within both models as shown in Fig. 13. The area measurement results are given in Table 9 as follow. Measurements done in two models are showed graphically as shown in Fig. 14.

Table 9
Area measurements carried out from both models for the same areas

First Study (Sivas) Area Measurements					
Observation No	**With GCPs(m²)**	**Without GCPs(m²)**	**Δi(m²)**	**Relative Error %**	**RMSE(m²)**
Flat Areas	2789.200	2788.100	1.100	0.040	**1.264**
	682.526	683.594	-1.068	0.160	
	1277.400	1278.700	-1.300	0.100	
Inclined	854.864	853.288	1.576	0.180	
Areas	115.021	113.810	1.211	1.050	
		mean	**1.251**	**0.306**	

6.1.4 Volume Measurements for Sivas

In order investigate the usability of model generated without GCPs in the volume measurement issue, 4 different rock's volumes were measured within both model as shown in Fig. 15.

In Photoscan, the "reference surface" to be used for the calculation of the volumes, can only be a plane. This surface can be defined in three ways:

1. as an inclined flat surface and interpolated by the vertices of the delimitation of the object (best fit plane).
2. as a horizontal flat surface with a medium height determined by the heights of the vertices of the delimitation of the object (mean level plane);
3. as a horizontal flat surface at a reference height determined by the user (custom level plane).

The results of volume measurements given as Table 10 and Fig. 16.

Table 10
Volume measurements and RMSE

Fisrt Study (Sivas) Volume Measurement					
Observation No	**With GCPS (m^3)**	**Without GCPs(m^3)**	**Δi(m^3)**	**Relative Error %**	**RMSE(m^3)**
1	24.119	22.478	1.641	6.800	**2.301**
2	101.393	104.088	-2.695	2.660	
3	52.881	54.043	-1.162	2.200	
4	409.243	406.101	3.142	0.80	
		mean	**2.160**	**3.115**	

6.2 Artvin Area's Experimental Studies (Second Study Area)

In this model measurements of length, area and volume is done as in last two model and the results of measurement done over both model (with and without GCPs) are given in Tables 11.

6.2.1 Length Measurements

Lengths of regions with different shapes was measured for intended goal as shown in Fig. 17 and the measurements are given in Table 12. Graphical vision of length measurements as shown in Fig. 18.

Table 11
Measured length values

Third Study (Artvin) Lenght Measurements					
Observation No	**With GCPs(m)**	**Without GCPs(m)**	**Δi(m)**	**Relative Error %**	**RMSE(m)**
1	209.522	209.303	0.219	0.100	**0.153**
2	69.293	69.199	0.094	0.140	
3	58.667	58.552	0.115	0.200	
		Mean	**0.143**	**0.147**	

6.2.2 Area Measurements of Second Study Area (Artvin)

Areas of different objects are measured in both model and as given in Fig. 19. Graphically representation of area measurement as given in Fig. 20.

Table 12
Area measurements from both model

Third Study (Artvin)(Bitlis) Area Measurements					
Observation No	**With GCPs(m²)**	**Without GCPs(m²)**	**Δi(m²)**	**Relative Error %**	**RMSE(m²)**
1	215.045	212.828	1.207	0.560	**1.726**
2	27.967	26.494	1.473	5.270	
3	65.567	63.263	2.304	3.510	
		Mean	**1.661**	**3.113**	

6.2.3 Volume Measurements of Second Study Area (Artvin)

Volumes of different objects are measured for intended goal (usability investigation of model generated without GCPs) as shown Fig. 21.

The measured values of volumes are given in Table 13.

Table 13
Volume measurements and RMSE

Third Study (Artvin) Volume Measurement					
Observation No	**With GCPS (m³)**	**Without GCPs(m³)**	**Δi(m³)**	**Relative Error %**	**RMSE(m³)**
1	2129.885	2118.759	11.126	0.520	**7.061**
2	161.364	158.123	3.241	2.010	
3	779.396	775.485	3.911	0.502	
		mean	**6.093**	**1.011**	

The volumes measured over both model are given graphically in Fig. 22.

7. Discussion And Conclusion

These studies were conducted to investigate the usability of 3D photogrammetric models produced without using any GCPs (ground control points), for this goal two different areas were modeled, each twice once with GCPs and once without GCPs. For the mentioned goal lengths, areas and volumes of same areas were measured on both models. The results obtained from the models generated with GCPs were accepted as true values (reference values) and the results obtained from models generated without GCPs were compared to them and the relative errors as well as RMSE were also calculated and given in tables above.

7.1 Length Measurements Assessment

Results from length measurement provided various level of success. The accuracy of each measurement was assessed by comparing reference data (obtained from model with GCPs) to estimations determined

through photogrammetric models without GCPs. In first study area (Sivas) length measurements of three types of terrain (flat, sloping and rocky terrain) were conducted. As seen in Table 5 the errors of length measurement in flat areas are less than the errors of the inclined areas, similarly the length measurement errors of inclined areas are less than the errors of rocky areas. It is important to know that some objects used for length measurement especially in inclined areas were in close proximity to other objects and were complex enough. But overall first study area exhibited very promising results in length measurement with a relative error of less than 1% and RMSE of 0.139m and this result is accurate enough.

In second study area (Artvin) length of various places were measured. The relative error value is 0.15% and the RMSE is 0.153m and these errors are also within acceptable error limits.

Based on analysis of length measurements performed in models generated with GCPs and those performed over models without GCPs no marked difference was found. The majority of relative error calculations was less than 1%. The influence of object shape, size and configuration on the accurate estimation of length obtained from models without GCPs were examined in this study. As seen in Table 5, the areas with greater slope and complexity contain more errors than the flat areas. In first study the flat area has a majority relative error of 0.10% whereas inclined area has a majority relative error of 0.20% and finally length measured in the rocky area has a relative error of 0.36%. The rocky area has the highest error as well as the most complex structure in the first study area. So as result the higher the inclination and the complexity of the object, the greater the error

The maximum relative error of length measurement among study area is 0.36% which is an acceptable length accuracy. Given the acceptable accuracy assessment in various fields it is possible to conclude that the photogrammetric models produced without GCPs are adequate for estimating lengths of objects for different engineering applications, some quantity estimations within civil engineering projects, as well as disciplines that do not require very high accuracy, while it may not be suitable for disciplines that require a very high level of accuracy (millimetric accuracy). According to the above descriptions, we can indicate that models generated without GCPs can be used for length measurement as an accurate length measurement tools.

7.2 Area Measurements Assessment

Area estimations show varying results. The accuracy of each estimation (measurement) was assessed by comparing reference data (obtained from model with GCPs) to estimations determined through photogrammetric models without GCPs.

In the area estimation, out of 8 areas measured within three study areas, five have a relative error of less than 1%. one of them has a relative error of less than 2% and one with a relative error of 3.51% and the last one contains the maximum relative error of 5.27%. The influence of the shape and size can be seen such as in length measurement. As seen in Table 6 of first study, the flat area has a majority relative error of 0.16% whereas the inclined area has a majority relative error of 1.05%. As said for the length, the higher the inclination and the complexity of the object, the greater the error.

7.3 Volume Measurement Assessment

Results of volume estimations obtained from two studies are convincing. Within the first study area (Sivas), the largest area exhibited a relative error of 0.8% and the maximum relative error of volume estimation is 6.8%. However the error looks to be a bit higher but absolute error is no more than 1.641m³.

The average relative error is calculated as 3.115% and RMSE is calculated as 2.301 m³ likely coming from the failure of the software to model the object structure properly.

Similarly within volume estimation of second study a maximum relative error of 2.01% has been identified with an RMSE of 7.061. It should be noted that the objects with the least accurate results have poor photo coverage, which sometime cause by the location of the object which is in the edge of the study area as well as insufficient image overlap and sometimes due to external factors. The errors can be reduced considering these factors.

7.4 Conclusions

Based upon the obtained results, several conclusions can be made as well as the decision to accept or reject the usability of models produced without GCPs. Considering the errors calculated above, the following conclusions are made pertain to the ability of photogrammetric models with no GCPs.

- Photogrammetric models generated with no GCPs are usable for different engineering applications.
- The photogrammetric models produced with no GCPs can be used as an accurate length measurement tool within modelled area.
- A relative error of 0.12% in first study area (Sivas) and 0.143% in second study area (Artvin) is obtained.
- Photogrammetric models with no GCPs can be used as an accurate area measurement tool within modelled area.
- Relative error in the case of area measurement of first study area (Sivas) is %0.306 and relative error for second study area (Artvin) is 3.11%.
- Photogrammetric models with no GCPs can calculate accurate volume of objects or/and areas with different shapes and slopes.
- A 3.115% relative error of volume measurement is calculated for first study area (Sivas), this value is 1.01% for second study area (Artvin).
- The length measurement within the flat areas of the model is more accurate than the measurement done within the inclined or rocky areas.
- The area measurements done in flat areas are also more accurate than those done in inclined area
- The area measurement of the object with smooth shapes are more accurate than the areas having complex shapes.
- The volume measurement's accuracy is based upon the identified base surface, if the surface is identified accurately, there is no effect of the shape or slope.
- The studies above are conducted in two areas with different characteristics such as elevation altitude above sea level, different climate conditions, different work area topographies, different flight planes and etc, but the results, the accuracies the relative errors and the absolute errors of these models are

about the same. As a result, it can be indicated that the above principles (usability of models with no GCPs) are acceptable and applicable for every conditions.

Declarations

Declaration of Conflicting Interests

None of the authors of this paper has a financial or personal relationship with other people or organisations that could inappropriately influence or bias the content of the paper. No competing interests are at stake and there is no conflict of interest with other people or organisations that could inappropriately influence or bias the content of the paper.

The authors declared no potential conflicts of interest with respect to the research, authorship, and/or publication of this article.

Funding

The authors received no financial support for the research, authorship and/or publication of this article.

References

1. Yastikli, N. Documentation of cultural heritage using digital photogrammetry and laser scanning. *Journal of Cultural Heritage.* **8** (4), 423–427 (2007).
2. McCarthy, J. Multi-image photogrammetry as a practical tool for cultural heritage survey and community engagement. *Journal of Archaeological Science.* **43**, 175–185 (2014).
3. Berni, J. A., Zarco-Tejada, P. J., Suárez, L. & Fereres, E. Thermal and narrowband multispectral remote sensing for vegetation monitoring from an unmanned aerial vehicle. *IEEE Transactions on geoscience and Remote Sensing.* **47** (3), 722–738 (2009).
4. Xiang, H. & Tian, L. Development of a low-cost agricultural remote sensing system based on an autonomous unmanned aerial vehicle (UAV). *Biosystems engineering.* **108** (2), 174–190 (2011).
5. Jauregui, L. M. & Jauregui, M. Terrestrial photogrammetry applied to architectural restoration and archaeological surveys. *International Archives of Photogrammetry and Remote Sensing.* **33** (B5/1), 5401–5405 (2000).
6. Bianchi, G. *et al.* Integrated Survey For Architectural Restoration: A Methodological Comparison Of Two Case Studies.*International Archives of the Photogrammetry, Remote Sensing & Spatial Information Sciences*, *41*, (2016).
7. Kucukkaya, A. G. Photogrammetry and remote sensing in archeology. *Journal of Quantitative Spectroscopy and Radiative Transfer.* **88** (1–3), 83–88 (2004).
8. Guidi, G. *et al.* A multi-resolution methodology for the 3D modeling of large and complex archeological areas. *International Journal of Architectural Computing.* **7** (1), 39–55 (2009).

9. Patikova, A. Digital photogrammetry in the practice of open pit mining. *Int. Arch. Photogramm. Remote Sens. Spat. Inf. Sci.* **34**, 1–4 (2004).
10. Sheng, Y. H., Yan, Z. G. & Song, J. L. Monitoring technique for mining subsidence with digital terrestrial photogrammetry. *Zhongguo Kuangye Daxue Xuebao(Journal of China University of Mining & Technology).* **32** (4), 411–415 (2003).
11. Murfitt, S. L. *et al.* Applications of unmanned aerial vehicles in intertidal reef monitoring. *Sci Rep.* **7**, 10259 (2017).
12. Yalcin, G. & Selcuk, O. 3D city modelling with Oblique Photogrammetry Method. *Procedia Technol.* **19**, 424–431 (2015).
13. Danahy, J. *In Automatic extraction of man-made objects from aerial and space images (II)*pp. 357–366(Birkhäuser, Basel, 1997). A set of visualization data needs in urban environmental planning & design for photogrammetric data
14. Döner, F. & Bıyık, C. Management of three dimensional objects in spatial database. *Chamber of Survey and Cadastre Engineers Geodesy and Geoinformation Magazine.* **100**, 27 (2009).
15. Yılmaz, H. M. *et al.* Created Tree Dimensional Model of Aksaray University Campus with Unmanned Aerial Vehicle. *Journal of Geomatics.* **3** (2), 103–1107 (2018).
16. Choudhury, M. A. M. *et al.* May. Photogrammetry and Remote Sensing for the identification and characterization of trees in urban areas. In Journal of Physics: Conference Series (Vol. 1249, No. 1, p. 012008). IOP Publishing(2019).
17. Wu, B., Xie, L., Hu, H., Zhu, Q. & Yau, E. Integration of aerial oblique imagery and terrestrial imagery for optimized 3D modeling in urban areas. ISPRS journal of photogrammetry and remote sensing. 2018 May 1;139:119 – 32, (2018).
18. Goetz, J. & Brenning, A. Quantifying uncertainties in snow depth mapping from structure from motion photogrammetry in an alpine area.*Water Resources Research*, (2019).
19. Chudley, T. R., Christoffersen, P., Doyle, S. H., Abellan, A. & Snooke, N. High-accuracy UAV photogrammetry of ice sheet dynamics with no ground control. *Cryosphere.* **13**, 955–968 (2019).
20. Casella, V. & Franzini, M. Modelling Steep Surfaces by Various Configurations of Nadir and Oblique Photogrammetry. ISPRS Annals of Photogrammetry,Remote Sensing & Spatial Information Sciences, 3(1), (2016).

Figures

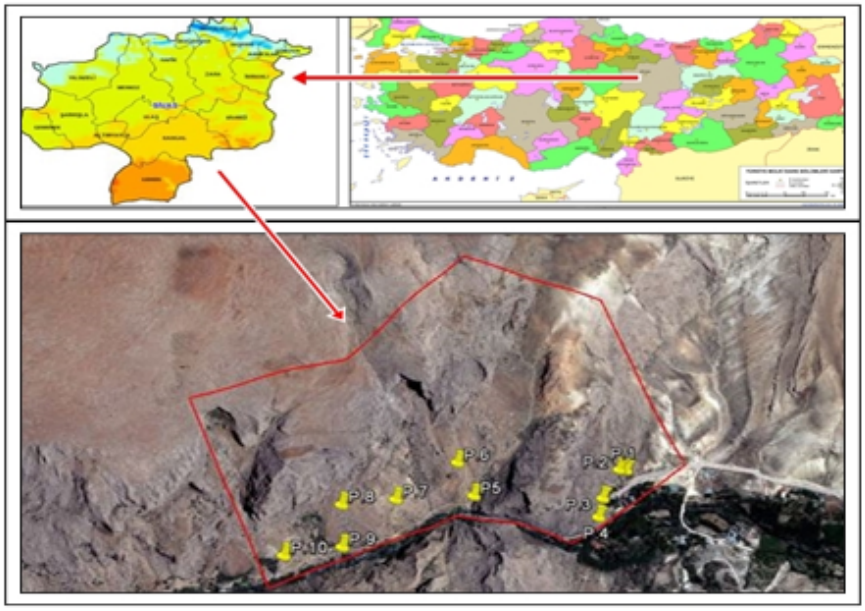

Figure 1

First Study area Sivas, Gürün, Şuğul Canyon, Turkey. Note: The designations employed and the presentation of the material on this map do not imply the expression of any opinion whatsoever on the part of Research Square concerning the legal status of any country, territory, city or area or of its authorities, or concerning the delimitation of its frontiers or boundaries. This map has been provided by the authors.

Figure 2

DJI Phantom 4Pro model UAV and CHC X91 model RTK-GNSS receiver used for data acquisition

Figure 3

Marking and measuring GCPs

Figure 4

Phantom 4Pro UAV camera

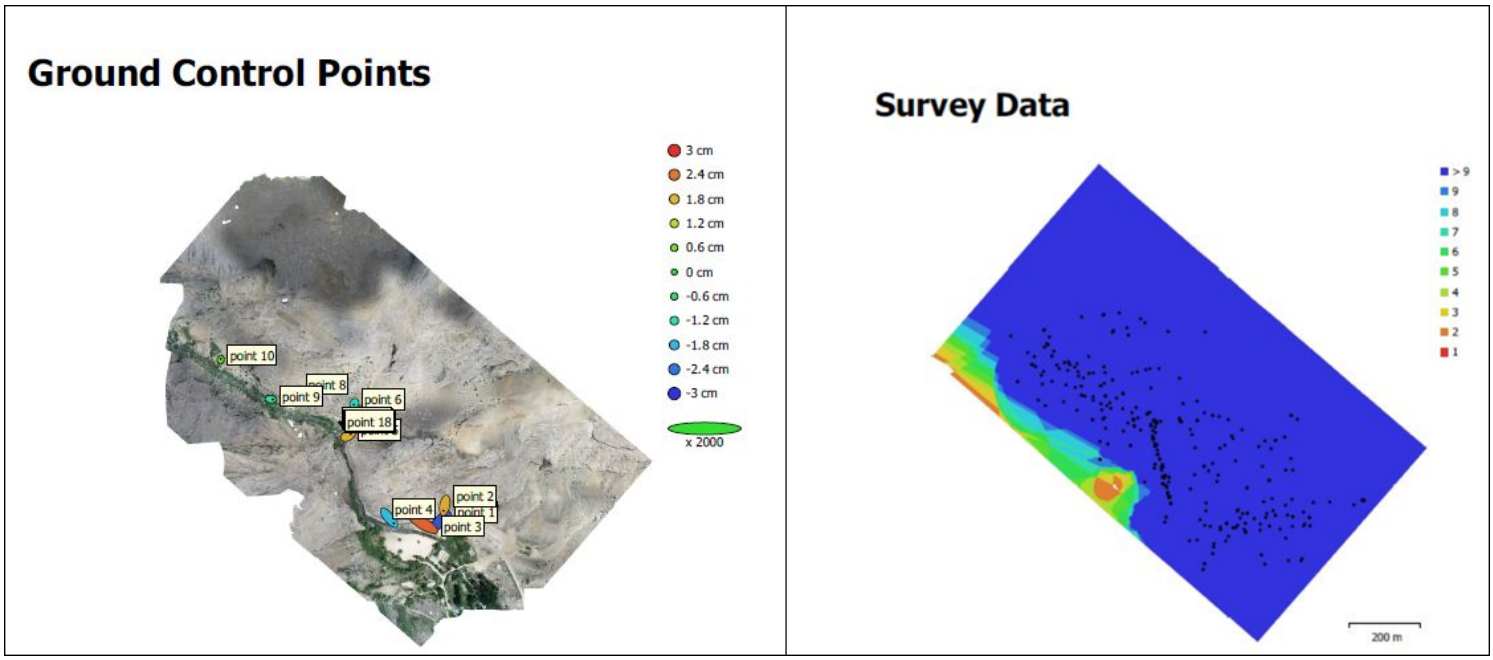

Figure 5

GCP positions, image overlaps and camera calibration.

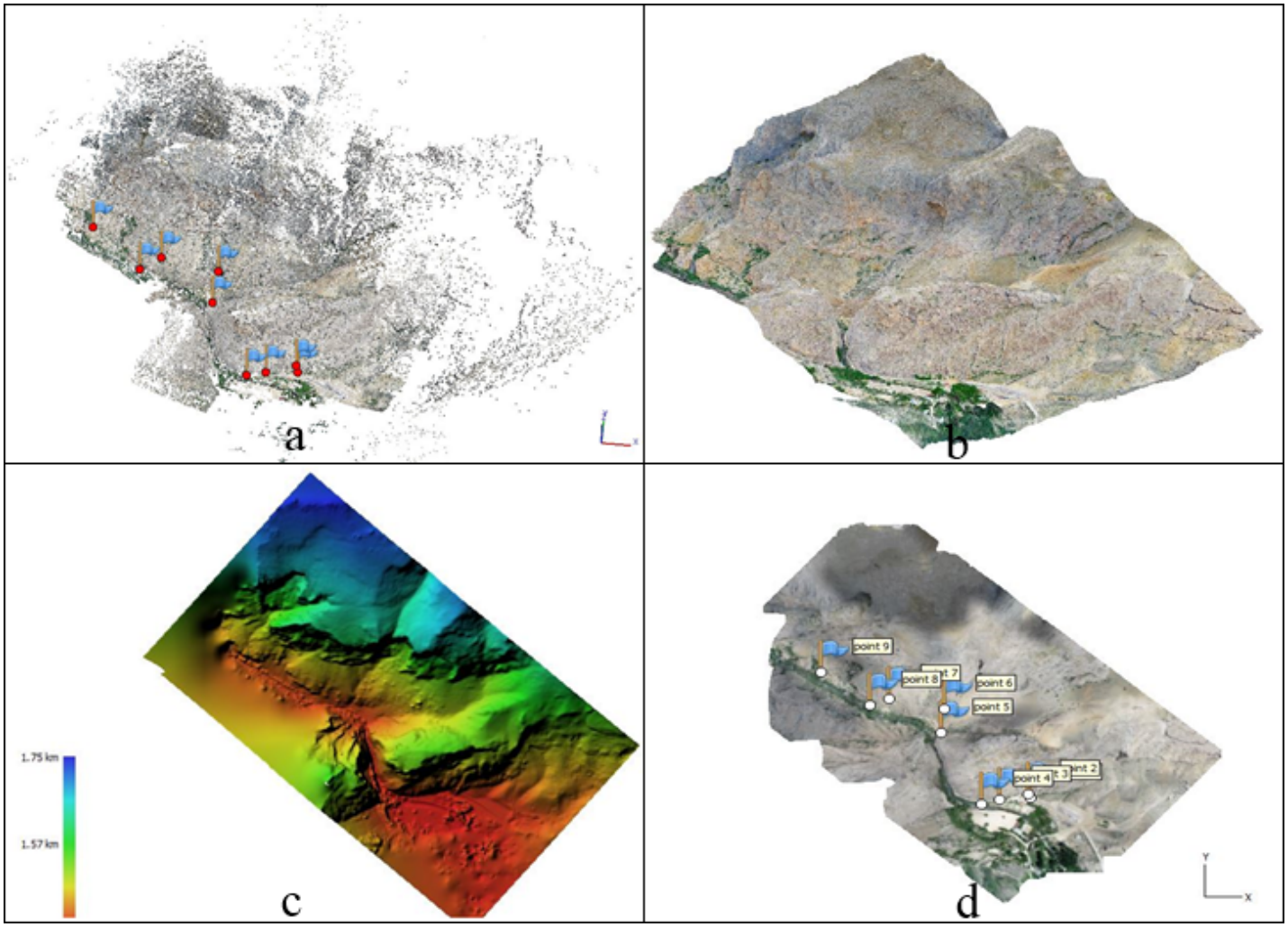

Figure 6

Results of photogrammetric evaluation a) Tie Points b) 3D model c) Digital Elevation Model d) Orthophoto

Figure 7

Second Study area a) Turkey b) Artvin b) Artvin Dam. Note: The designations employed and the presentation of the material on this map do not imply the expression of any opinion whatsoever on the part of Research Square concerning the legal status of any country, territory, city or area or of its authorities, or concerning the delimitation of its frontiers or boundaries. This map has been provided by the authors.

Figure 8

Equipment used to obtain datasets.

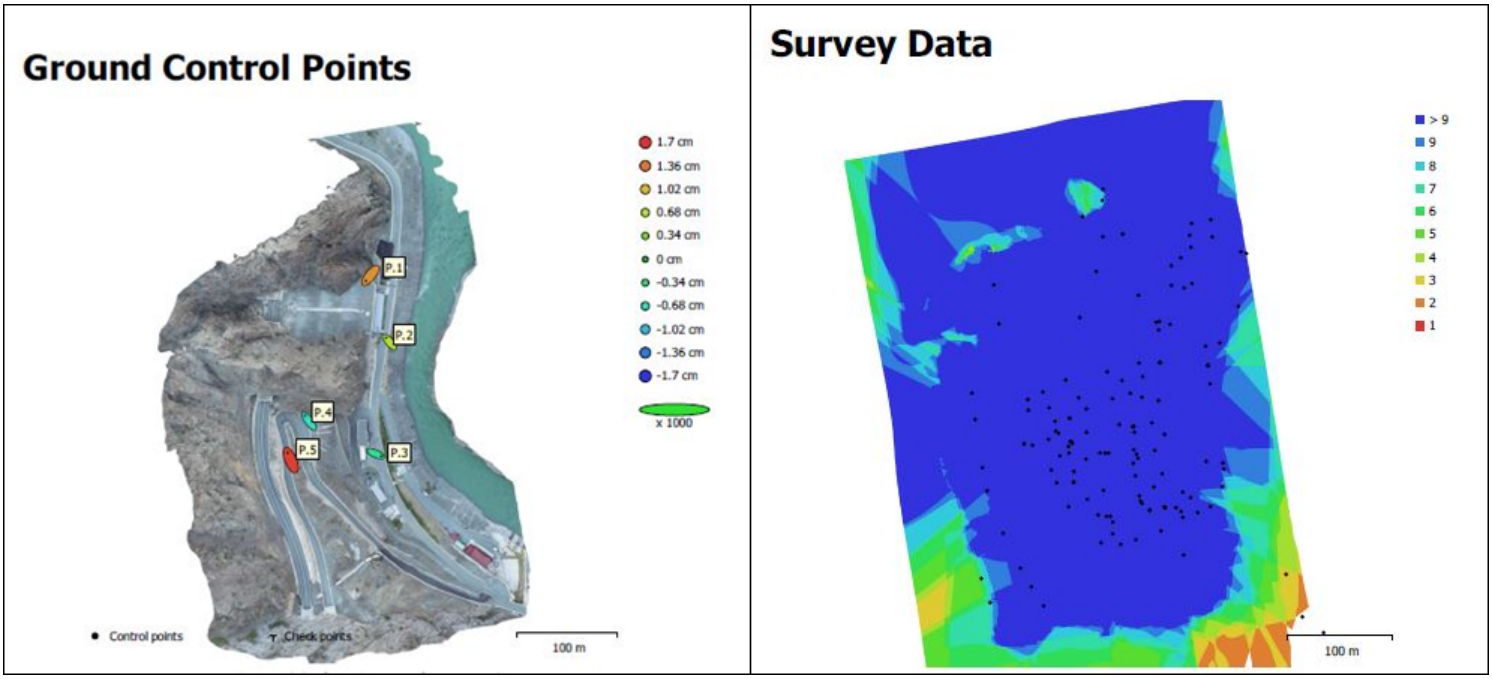

Figure 9

GCPs positions and overlaps

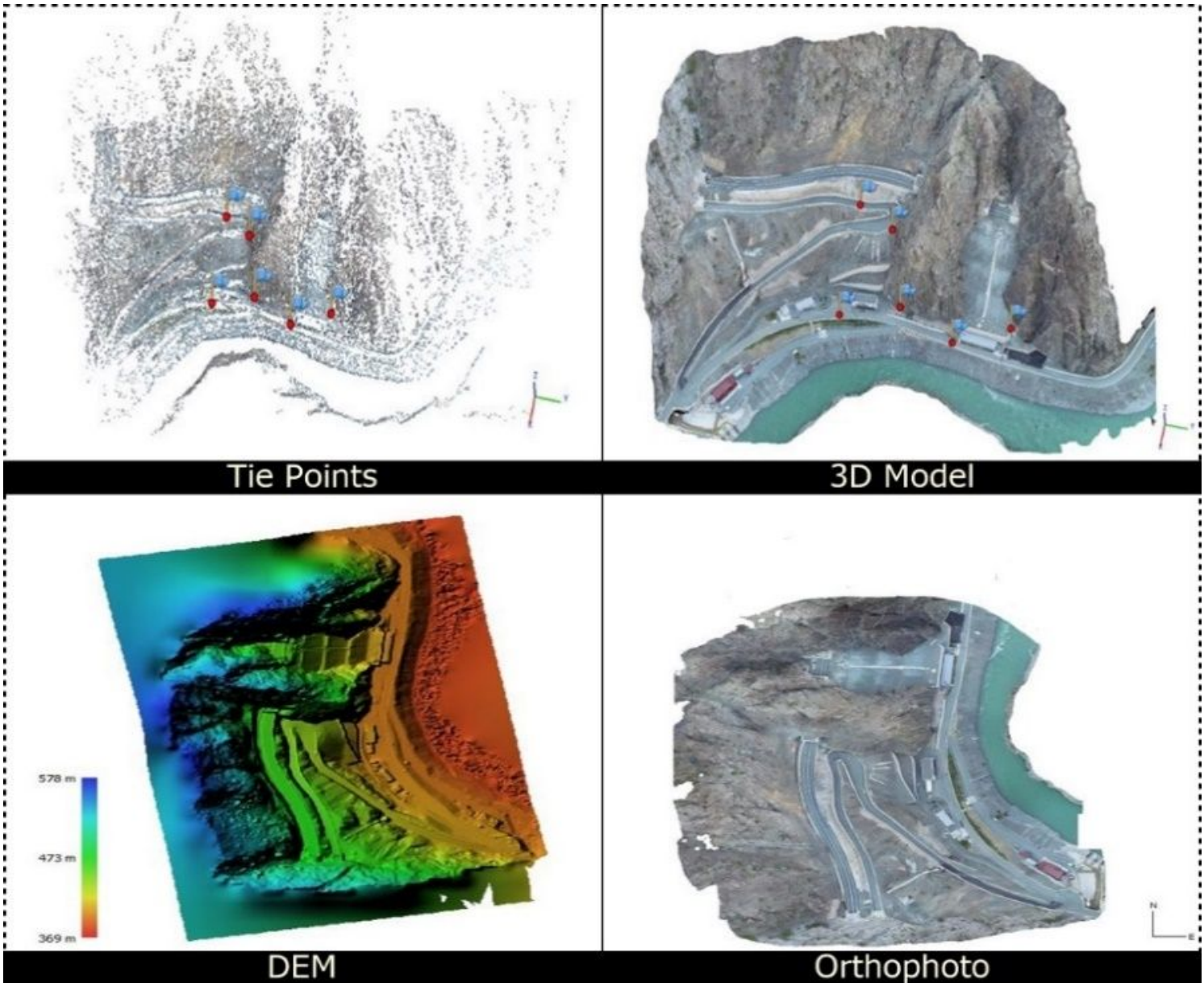

Figure 10

Tie Points, 3D model, Digital Elevation Model and Orthophoto

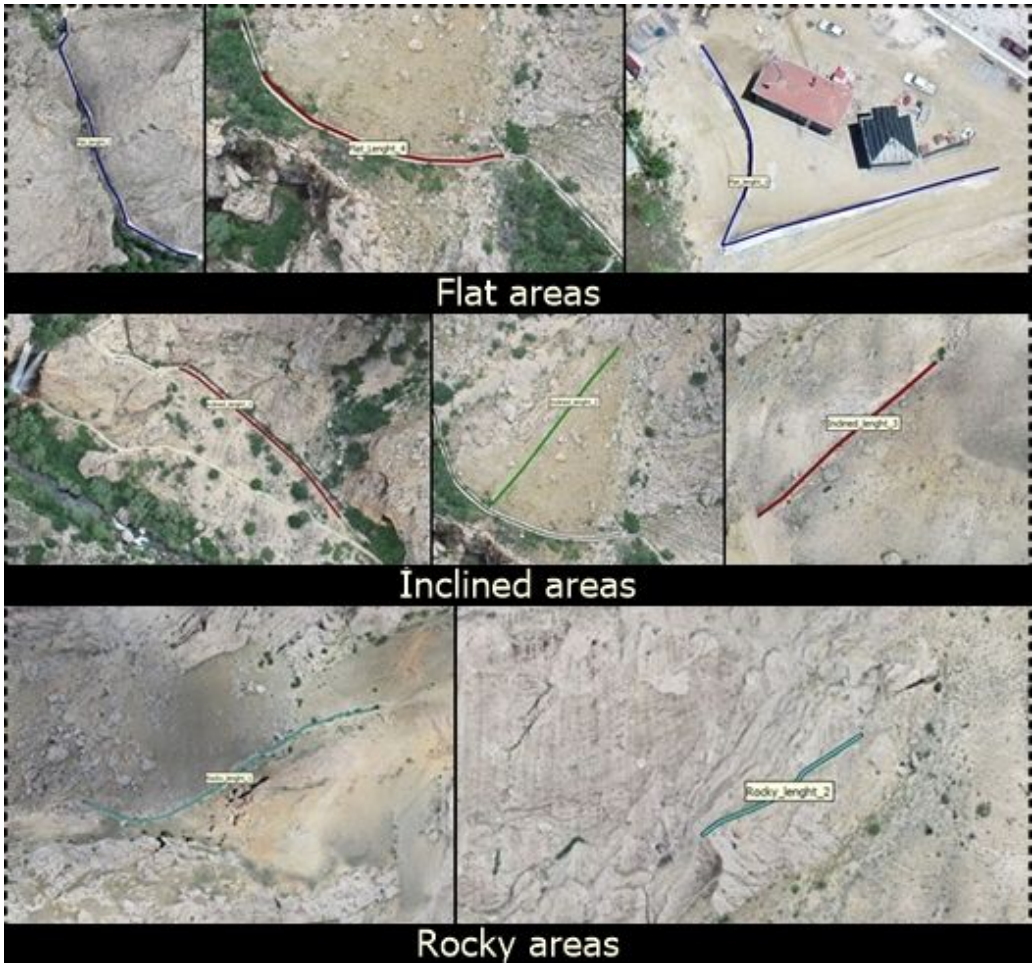

Figure 11

Length measurements of areas with different topography

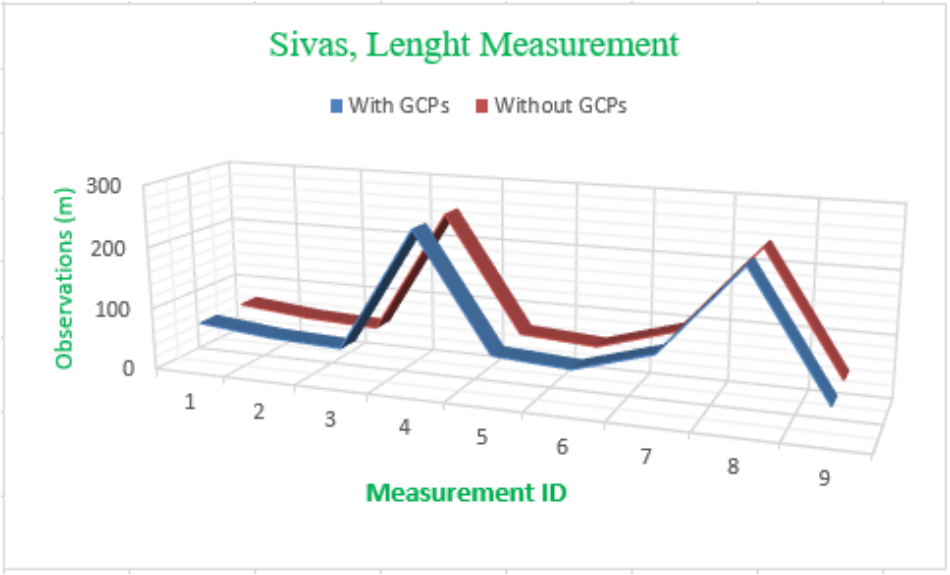

Figure 12

Measurements done in two models are graphically indicated

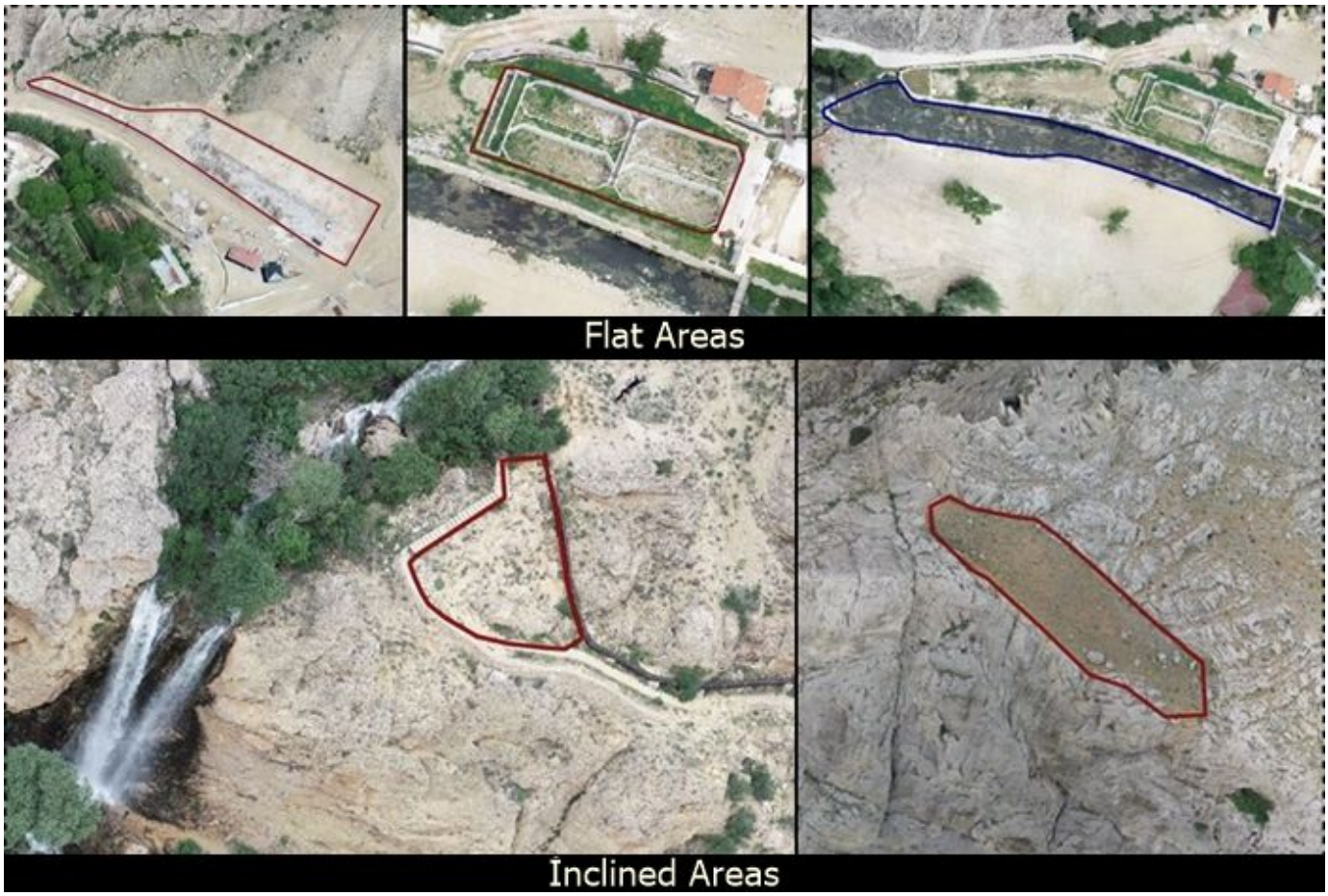

Figure 13

Area measurements done over both model

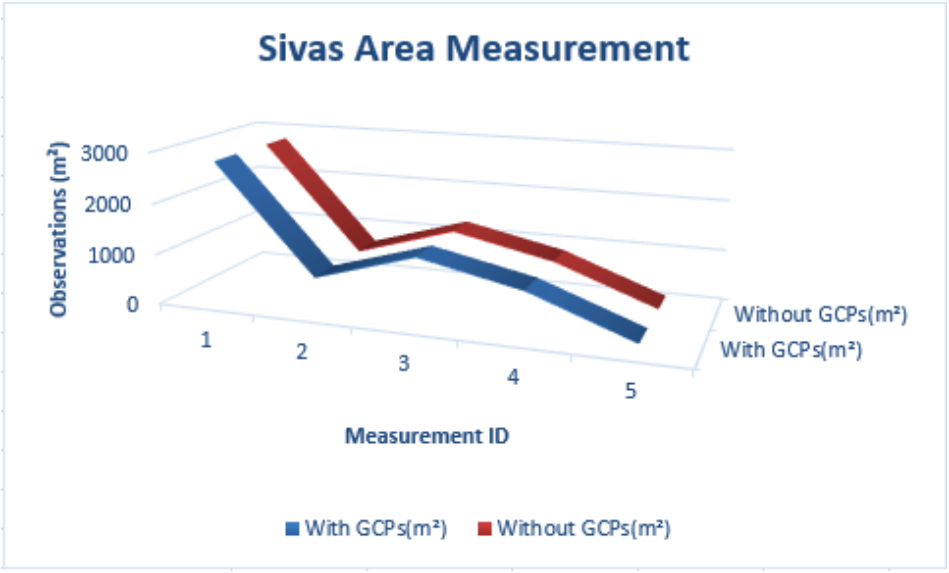

Figure 14

Measurements done in two models are showed graphically

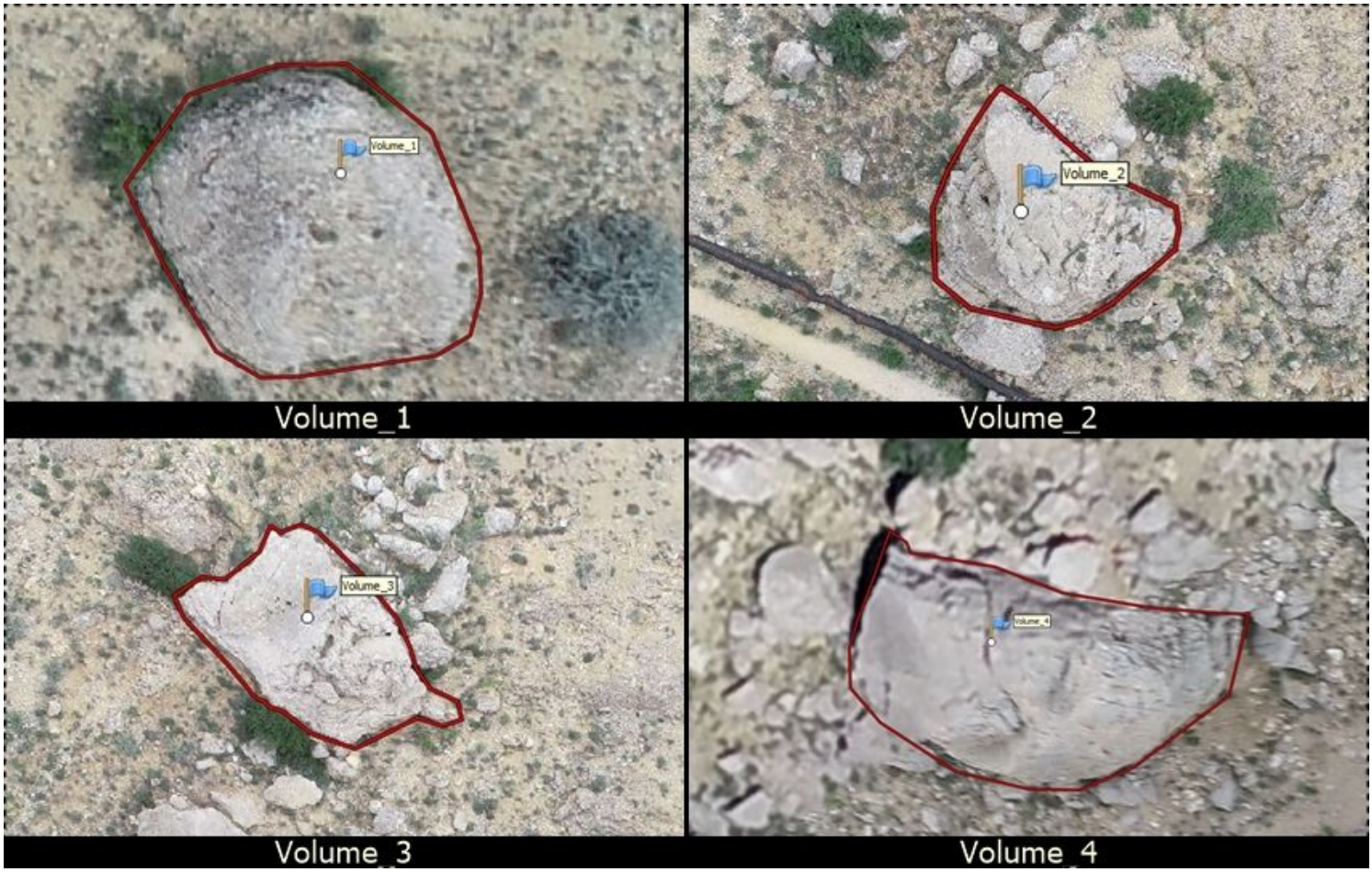

Figure 15

Volume measurements of 4 rock done within both model

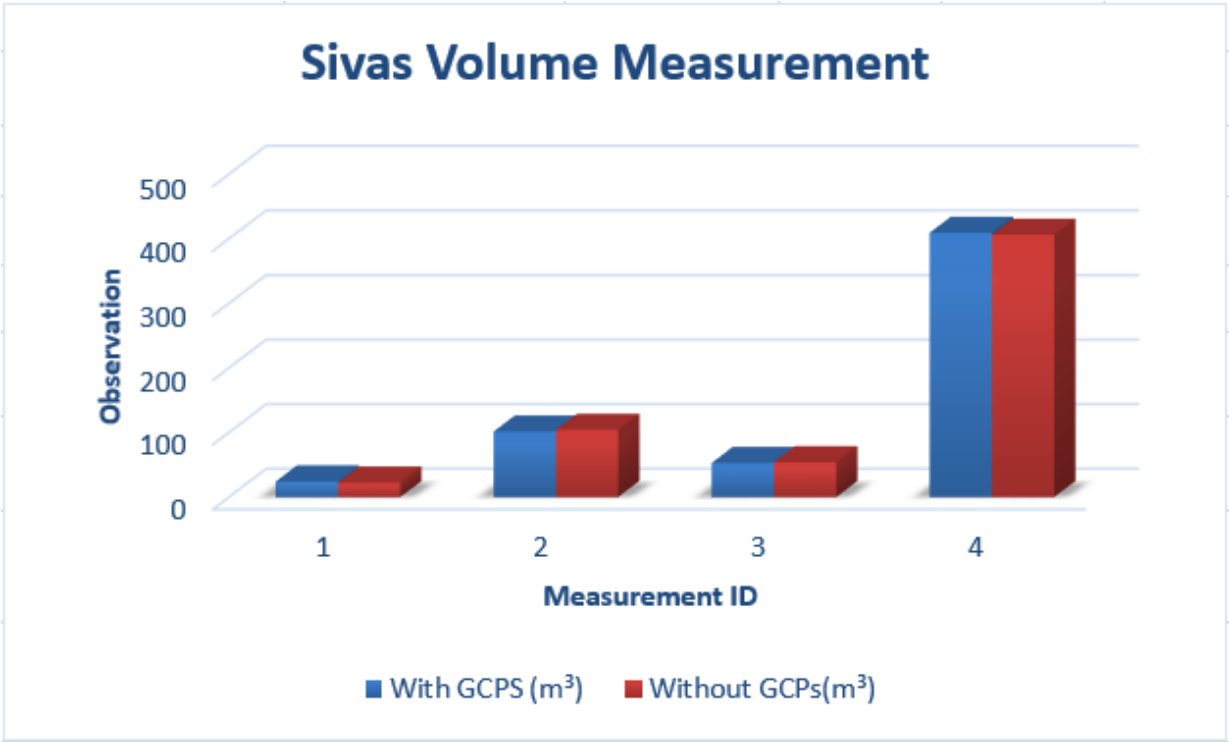

Figure 16

Volume measurements are shown graphically

Figure 17

Length measurements for third study area

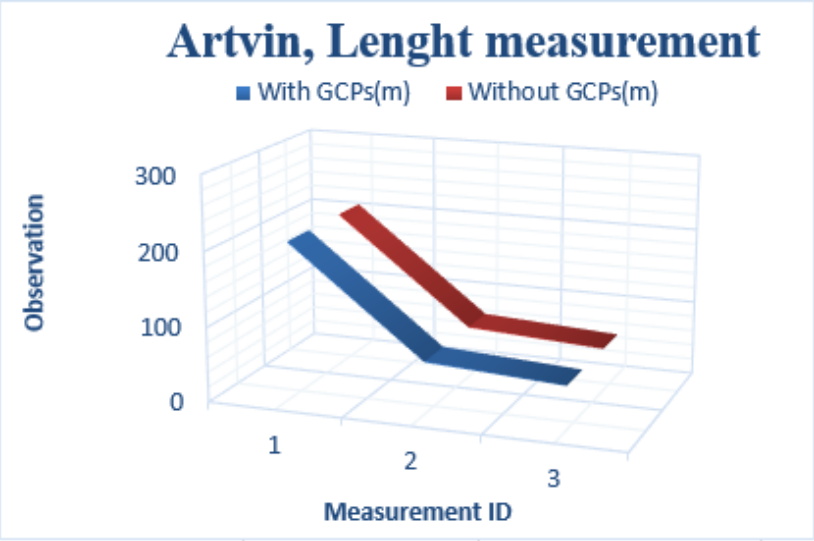

Figure 18

Graphical vision of length measurements

Figure 19

Areas measured in two models

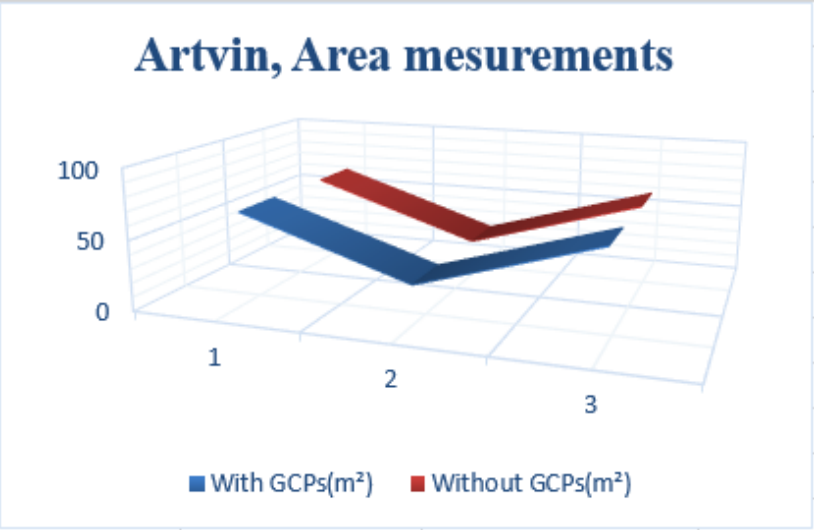

Figure 20

Graphically representation of area measurements

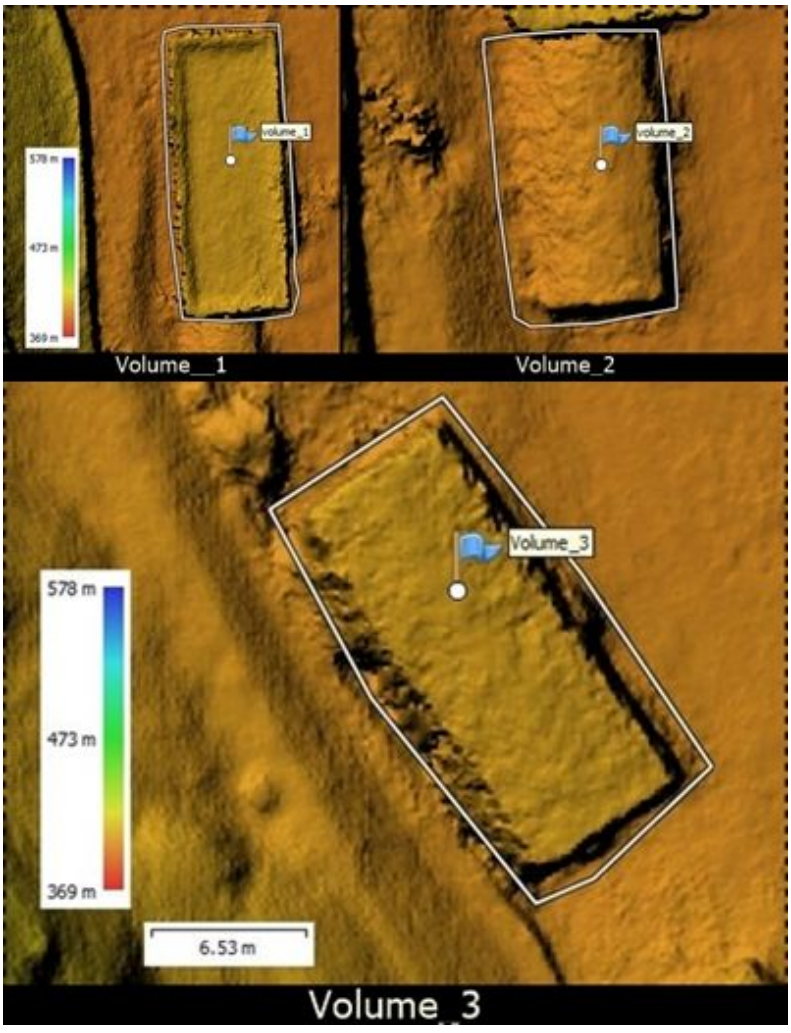

Figure 21

Volume measurements

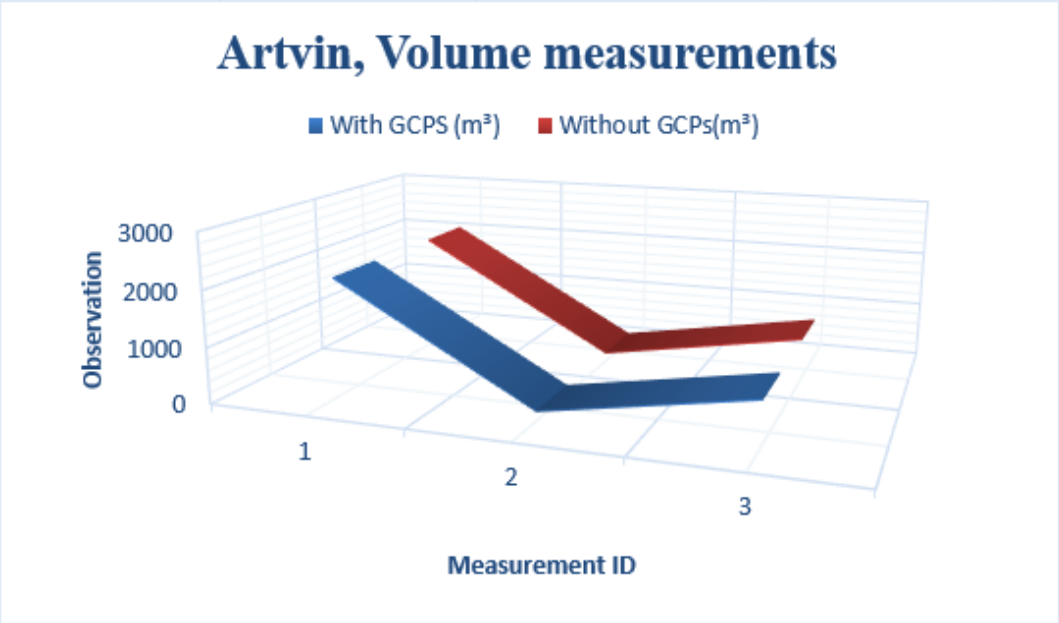

Figure 22

Graphic representation of volume measurements